

## Semiconductor nanowires

DOI: 10.1002/sml.200500094

**Top-Down Fabrication of Semiconductor Nanowires with Alternating Structures along their Longitudinal and Transverse Axes\*\****Yugang Sun, Rachel A. Graff, Michael S. Strano, and John A. Rogers\**

Semiconductor nanostructures in general, and nanowires in particular, are of interest because of their unique properties (e.g., quantum effect, high mechanical flexibility, and so on)<sup>[1,2]</sup> and the ability to tailor these properties by controlling dimension, morphology, composition, crystallinity, and surface modification. For example, CdSe nanorods (with a

length of 29 nm and diameter of 4 nm) covered with two monolayers of ZnS exhibit a high quantum yield when they are irradiated by excitation light. Selective attachment of gold dots at the ends of nanorods significantly quenches their fluorescence.<sup>[3]</sup> Reducing the lateral dimensions of the wires increases their mechanical flexibility and makes them a promising printable type of semiconductor for flexible, high-performance macroelectronic devices with large area.<sup>[4]</sup> Furthermore, semiconductor nanostructures that incorporate complex alternating structures, that is, superlattices, offer additional interesting properties and potential applications.

Several synthetic “bottom-up” approaches can be used to prepare such superlattices. For instance, the vapor-liquid-solid (VLS) process,<sup>[5]</sup> which is the most successful approach for synthesizing single-crystalline semiconductor nanowires, provides a convenient way to prepare junctions (formed between two different semiconductor segments) within nanowires by alternating the vapor-phase semiconductor reactants during growth. In this way, nanowires made of superlattices from group III–V (e.g., GaP/GaAs and InP/InAs)<sup>[6,7]</sup> and group IV (e.g., Si/SiGe)<sup>[8]</sup> materials have been successfully synthesized. An alternative method demonstrated by Alivisatos et al. can produce semiconductor nanorods and branched structures with hetero-compositions in homogeneous solutions by sequential growth of semiconductor dots and rods of different materials (e.g., CdSe/CdTe).<sup>[9]</sup> In both classes of experiments, the different materials had similar crystallinities and lattice parameters. Anisotropic growth of a metal onto a semiconductor nanowire (or a semiconductor on a metal nanowire), however, represents a challenge. Recent work reported by Banin et al. showed that gold dots could selectively grow onto the tips of semiconductor nanorods (or tetrapods) by reducing AuCl<sub>3</sub> with dodecylamine in the presence of dedecyldimethylammonium bromide in the toluene solution of semiconductor colloids.<sup>[3]</sup> Semiconductor components, however, might be difficult to grow on the gold tips to generate superlattices with more repeatable units. Lieber and co-workers recently developed an effective approach to prepare metal/semiconductor nanowire heterostructures by transforming specific sections of a semiconductor Si nanowire, synthesized via the VLS process, into metallic nickel silicide through photolithography and high-temperature annealing.<sup>[10]</sup> Although it has not been demonstrated, it is possible that the dimensions and morphologies (i.e., cross sections), could also be modulated within wires formed using these “bottom-up” procedures.

Here, we report a “top-down” approach that combines multiple lithographic steps and anisotropic chemical etching processes (or deposition of other materials), to produce GaAs nanowires with controlled properties along their longitudinal and transverse axes. Our previous work demonstrates that arrays of GaAs nanowires with triangular cross sections can be prepared using a specially designed pattern as an etch mask.<sup>[11]</sup> Here, it is shown that these wire arrays can be conveniently processed by photolithography and further etching (or metallization) to generate GaAs wires with complex structures. We illustrate this strategy to produce

[\*] Dr. Y. Sun, Prof. J. A. Rogers  
Department of Materials Science and Engineering  
Frederick Seitz Materials Research Laboratory and Beckman  
Institute, University of Illinois at Urbana-Champaign  
Urbana, IL 61801 (USA)  
Fax: (+1) 217-333-2736  
E-mail: jrogers@uiuc.edu

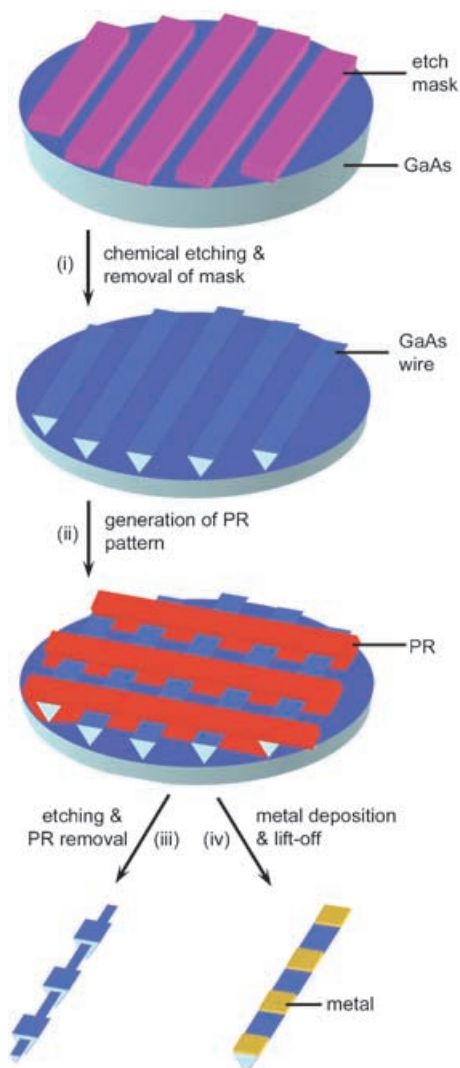
R. A. Graff, Prof. M. S. Strano  
Department of Chemical and Biomolecular Engineering  
University of Illinois at Urbana-Champaign  
Urbana, IL 61801 (USA)

[\*\*] This work was supported by the DARPA-funded AFRL-managed Macroelectronics Program (FA8650-04-C-7101). It was also partially supported by the U.S. Department of Energy under grant DEFG02-91-ER45439 and by the National Science Foundation under grant NSF-DMII 03-28162. The fabrication and measurements were carried out using the facilities located in the Microfabrication Laboratory and Center for Microanalysis of Materials of Frederick Seitz Materials Research Laboratory, which are supported by Department of Energy.

Supporting information for this article is available on the WWW under <http://www.small-journal.com> or from the author.

wire arrays that have controlled variations in dimension, composition, and morphology.

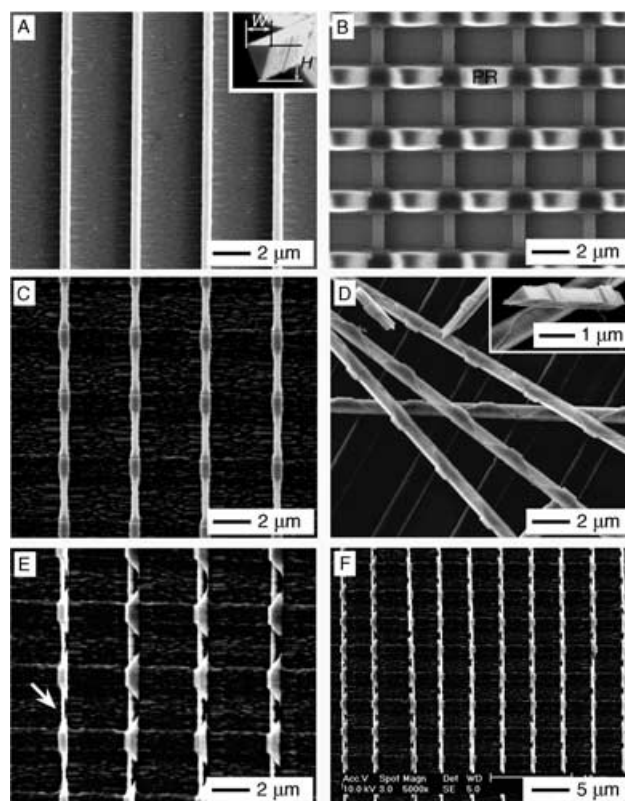
Figure 1 summarizes the steps for producing certain classes of structures. First, GaAs wire arrays are prepared by anisotropically etching a GaAs(100) wafer patterned



**Figure 1.** Schematic diagram for fabricating GaAs wires with alternating dimensions or compositions along their longitudinal axis. The steps include: i) preparing an array of GaAs wires with a triangular cross section from a GaAs(100) wafer patterned with mask stripes along the  $(0\bar{1}1)$  direction and anisotropically etched in an aqueous solution consisting of  $\text{H}_3\text{PO}_4$  (85 wt%),  $\text{H}_2\text{O}_2$  (30 wt%), and  $\text{H}_2\text{O}$  (1:13:12 in volume); ii) patterning the resultant wire array (after removal of the etch mask stripes) with photoresist lines perpendicular to the orientation of the GaAs wires; and iii) etching the GaAs wires using the photoresist as a mask to generate wires with alternating widths, or iv) depositing metals through the photoresist pattern to create GaAs wires with segments alternating in composition.

with mask stripes ( $\text{SiO}_2$  or photoresist) along the  $(0\bar{1}1)$  direction (step i).<sup>[11,12]</sup> When the stripes are surrounded by broad features of the mask material, chemical etching produces GaAs wires with ends that connect to the mother wafer. These connection points pin the GaAs wires at their

ends; they hold the wires in the positions defined by the pattern of mask stripes even when the wires are completely undercut. Resist patterns are then defined (in some cases by conventional photolithography) onto the pinned wire arrays (step ii). These resist features serve as masks for modifying the properties of the exposed segments of the wires. We demonstrate here three possibilities: 1) Etching exposed sections of the wires and then removing the resist to produce GaAs wires with alternating widths (step iii), 2) depositing materials (e.g., metals) onto the exposed sections to form GaAs wires with segments composed of alternating compositions (step iv), and, as described in detail in a following section, 3) anisotropically etching exposed regions to form wires with complex cross-sectional shapes.



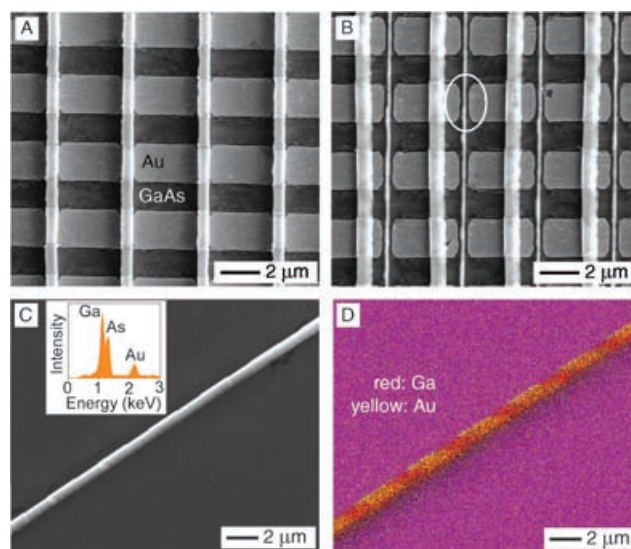
**Figure 2.** SEM images of samples obtained by etching 400 nm GaAs wires through  $\approx 1.8\text{-}\mu\text{m}$ -wide photoresist (PR) lines oriented perpendicular to the wire orientation: A) Parallel GaAs wires with widths of  $\approx 400$  nm on the mother wafer; B) a GaAs wire array covered with patterned photoresist lines oriented perpendicular to the wires; C) top-view and D) side-view SEM images of GaAs wires after etching the sample shown in (B) for 20 s; E, F) SEM images of wire arrays after etching the sample shown in (B) for 45 s.

Figure 2 shows scanning electron microscopy (SEM) images of GaAs wires before and after selective etching for different durations. Figure 2A shows an SEM image of an array of wires on a mother wafer as obtained by etching ( $\text{H}_3\text{PO}_4$  (85 wt%): $\text{H}_2\text{O}_2$  (30 wt%): $\text{H}_2\text{O}$  = 1:13:12 in volume) through masks of parallel  $\text{SiO}_2$  lines (with a width of  $\approx 2\text{ }\mu\text{m}$ ). Wires produced in this fashion have widths ( $W$ ) of  $\approx 400$  nm; they retain the alignment established by the

photolithography. The difference between the widths of the nanowires and the SiO<sub>2</sub> mask stripes reveals that the chemical etching generates undercutting along with vertical etching. The anisotropic etching continues even if the wires lift off from the mother wafer. As a result, the widths of the GaAs wires can be decreased down to 50 nm by controlling the etching time.<sup>[11]</sup> The inset gives an SEM image of a broken wire, clearly showing its triangular cross section. The height (*H*) of this wire (i.e., the perpendicular distance between the sharp ridge released from mother wafer and (100) top surface) is  $\approx 650$  nm. To produce more complex structures, the mother wafer is spin cast with a photoresist film that can be patterned into lines perpendicular to the orientation of GaAs wires, that is, along the (0 $\bar{1}$ 1) direction. Figure 2B shows a GaAs wire array covered with photoresist lines with widths of  $\approx 1.8$   $\mu\text{m}$  and spacings of  $\approx 2.2$   $\mu\text{m}$ . In this step, the thickness of the photoresist film must exceed the heights of the wires in order to generate continuous features. These photoresist lines serve as masks for etching the exposed sections of wires in the same etchant used to prepare the wires (Figure 2A). Figure 2C and D present SEM images of products obtained by etching samples shown in Figure 2B for 20 s and then removing the photoresist. These images show that GaAs wires with triangular cross sections and alternating widths along their longitudinal axis can be prepared. As shown in Figure 2C, the sections of the wires not coated with photoresist were etched anisotropically, with some undercut. The widths of these open sections were reduced, indicating that the side walls of each wire were also etched. Figure 2D shows a random assembly of several broken wires with their side walls facing the SEM detector. Unlike the uniform etching over the exposed (100) top surface, anisotropic etching of the side walls removes a layer of GaAs with a V-shaped profile. The inset shows that the triangular profile is retained during the thinning process. The angle between two side walls of the thinner section is similar to that of original wires, which indicates that the crystalline orientation of the newly generated surfaces are the same as that of the surface planes of the original wires. Such etching behavior might be ascribed to the combined effects of a high resistance of etching on the side walls and the intrinsic anisotropy of the etching. When a sample, such as that shown in Figure 2B, is soaked in etchant, etching initiates from the (100) top surface because this surface is more chemically active than the side surfaces. Because both edges have a higher probability of being etched than the middle part of the top surface of each wire, the vertical etching rate along side walls is higher than that of middle part. As a result, a thin layer of GaAs is peeled off from each side wall. According to the chemistry and crystallography involved in the anisotropic etching, a mesa-shaped profile rather than a reverse mesa is formed when mask lines are defined along the (0 $\bar{1}$ 1) direction.<sup>[13]</sup> The orientation-related etching behavior causes the side walls to be decorated with V-shaped notches. Longer etching times continue to shrink the segments exposed to the etchant, thereby increasing the ratio between thicknesses of two adjacent sections of each wire. Figure 2E and F show SEM images of a sample obtained by etching the GaAs wires shown in Figure 2B for

45 s, illustrating that the width of thinner sections (as indicated by the arrow) is  $\approx 120$  nm. The ratio between the widths of the thick and thin segments is  $\approx 3.4$ . Different lengths and spacings of these alternating width structures can be achieved easily by the use of appropriate photo-masks. For example, segments with lengths of  $\approx 5$   $\mu\text{m}$  were prepared with a mask consisting of parallel 5  $\mu\text{m}$  wide lines with spacings of 5  $\mu\text{m}$ . Figure S1 (see Supporting Information) shows SEM images of GaAs wires processed with this mask. Also, it is not necessary for each segment along the longitudinal axis of each wire to be the same.

Similar lithographic strategies can be used to achieve wires that vary in composition, by depositing functional materials onto their surfaces. For instance, the deposition of gold by electron beam evaporation on samples similar to that shown in Figure 2B, followed by liftoff of the photo-



**Figure 3.** Characterization of GaAs wires covered with alternating Au segments (thickness 40 nm): A, B) SEM images of a GaAs wire array on the mother wafer, with patterned Au stripes; C) SEM image of an individual GaAs wire with patterned Au stripes, resting on a Si wafer (inset: EDX spectrum of this wire, showing strong peaks for Ga, As, as well as Au); D) EDX mapping of Ga and Au over the wire shown in C).

resist in hot acetone generates a structure shown in Figure 3A. The GaAs mother wafer with the wire arrays is decorated with parallel Au stripes which have a thickness of 40 nm. The triangular cross sections of the GaAs wires and the collimated flux of Au from the evaporator yields Au stripes that terminate at the edges of each wire. Figure 3B shows that each Au stripe on the mother wafer is divided into individual segments (as indicated by the ellipse) after the GaAs wires are moved from their original positions. The (100) top surface of each GaAs wire is modified with Au stripes along the longitudinal axis. These wires can be released from the mother wafer, dispersed into a desired solvent (e.g., water) and deposited onto other desired substrates by solution casting. Figure 3C gives an SEM image of an individual wire on an ultraflat Si wafer, clearly show-

ing the alternating thicknesses along its longitudinal axis. The thicker segments are modified with Au films on the GaAs(100) surface. An energy-dispersive X-ray spectrum (EDX) of this wire exhibits a strong peak for Au as well as that of Ga and As. EDX mapping (see Figure 3D) of Au and Ga over this wire for 2 h confirms that each GaAs wire has alternating compositions (i.e., with or without a Au film) along its longitudinal axis.

Au films have unique surface plasmon resonance features,<sup>[14]</sup> which might couple with the optical responses of GaAs nanowires to modulate characteristics (e.g., peak shape or peak intensity) of their spectra. The metal can also

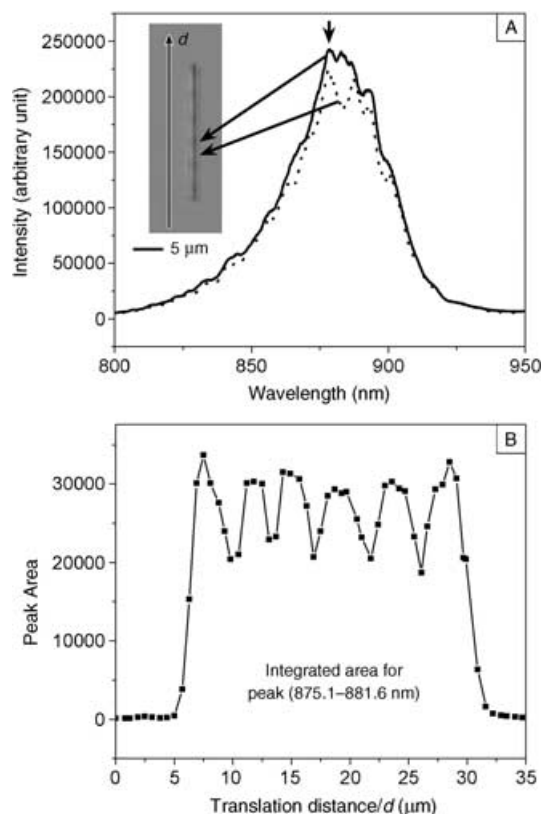


**Figure 4.** Photoluminescence of GaAs nanowires modified with alternating Au thin films (as shown in Figure 3): A) Spectral curves collected by illuminating the positions with (dotted curve) and without (solid curve) Au coverage; B) relationship between the area of the peak defined from 875.1 to 881.6 nm and the position along the longitudinal axis of the wire shown in the inset of (A).

quench photoluminescence and block incoming light that can stimulate light emission. Figure 4 shows the emission of an individual GaAs nanowire with Au stripes (the same as those shown in Figure 3), as excited with a confocal setup using a wavelength of 785 nm and a spot size of 0.6  $\mu\text{m}$ . The inset of Figure 4A presents an optical image of such a nanowire (length of  $\approx 25 \mu\text{m}$ ), clearly showing the alternating contrast associated with the Au. The bright and dark segments correspond to GaAs with and without the Au film, respectively. The emission spectra collected from GaAs nanowires modified with and without the Au film (Figure 4A) indicate that the deposition of a Au film on the sur-

face of the GaAs nanowires has no significant influence on the position of the emission bands. On the other hand, the Au films decrease the overall emission intensity as well as the relative intensities of the peaks. We calculated the area of the strongest peak (i.e., the peak from 875.1 to 881.6 nm as indicated by the arrow in Figure 4A) of a series of fluorescent spectra, which were obtained by scanning the laser beam along the longitudinal axis of the wire shown in Figure 4A. The dependence of the integrated peak area on the translation distance ( $d$ ) is presented in Figure 4B, indicating the periodic peak-to-valley variation. The result clearly shows that the periodicity, that is, the average distance between adjacent peaks (or valleys), is  $\approx 4 \mu\text{m}$ , which is consistent with the geometry shown in Figure 3. Integrated areas of other peaks also show the similar periodic variation along the longitudinal axis of this nanowire. This kind of composite wire structure might find use in optical applications. For example, the modulation of optical properties of these classes of GaAs nanowires makes them potentially useful as “barcode” structures.<sup>[15]</sup> In addition, the distinct surface chemistry of GaAs and Au enables one to easily modify these nanowires with different molecules for potential applications in various areas, such as sensing and photonics.

The same procedures can be used with other materials that can be patterned by liftoff. In addition to Au, magnetic materials (e.g., Ni) and semiconductor materials (e.g.,  $\text{TiO}_2$ ) were also patterned on GaAs nanowires. These wires can be thermally annealed to diffuse the deposited materials into the GaAs lattice to form alloys.<sup>[16]</sup> Solution-based materials, such as spin-on-glass<sup>[17]</sup> and thiol molecules,<sup>[18]</sup> can be spin-cast (or self-assembled) onto the substrate shown in Figure 2B to generate GaAs wires with alternating doping concentrations and surface chemistries along their longitudinal axis. This “top-down” approach provides a facile route to the large-scale fabrication of semiconductor nanowires with alternating properties (i.e., dimension, composition, and surface chemistry) along their longitudinal axes.

This technique can also be used to tune the cross section (or transverse axis) of GaAs nanowires from simple triangular to complex irregular profiles. For example, GaAs nanowires with a cross section exhibiting a doublet profile can be prepared via the process depicted in Figure 5. First, a GaAs nanowire array is fabricated through anisotropic etching of a GaAs(100) wafer using patterned  $\text{SiO}_2$  stripes as etch mask. This wire array can be transferred to a piece of flat poly(dimethylsiloxane) (PDMS) stamp, which is slightly oxidized in the atmosphere of oxygen plasma, based on the formation of covalent siloxane bonds (Si-O-Si) between the  $\text{SiO}_2$  mask stripes and the PDMS stamp (step i).<sup>[11]</sup> The surface of the PDMS stamp with GaAs wires is then spin cast with a layer of photoresist (PR) with a thickness less than the height ( $H$ ) of the GaAs wires, resulting in the formation of a photoresist film with very thin thickness at the sharp edges of the GaAs wires (step ii). Placing a pristine flat PDMS stamp (with a hydrophobic surface) against the photoresist film and peeling off this stamp will expose the sharp ridges of the GaAs wires because strong hydrophobic-hydrophobic interaction exists between the PDMS and

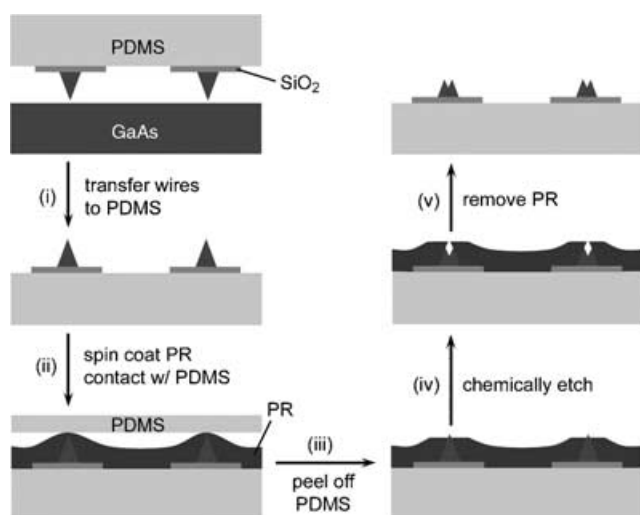


**Figure 5.** Schematic process for fabricating GaAs wires with doublet cross sections from wires with triangular cross sections, that is, a singlet profile. An array of GaAs wires with triangular cross sections is first fabricated from a GaAs wafer patterned with SiO<sub>2</sub> mask stripes through the process shown in Figure 1, step i. The resultant wire array is transferred to the surface of an oxidized flat PDMS stamp through chemical bonding formed between PDMS and SiO<sub>2</sub> (step i). The PDMS stamp with GaAs wires is spin-cast with a thin layer of photoresist (PR) and another pristine flat PDMS stamp is placed against the photoresist layer (step ii). Peeling off the new PDMS stamp exposes the ridges of the GaAs wires (step iii). Further chemical etching (step iv) and removal of the photoresist (step v) leave GaAs wires with a doublet cross section on the PDMS stamp.

the photoresist (step iii).<sup>[12]</sup> The photoresist film left on the PDMS stamp with GaAs wires is then hard-baked to become solid enough to serve as an etch mask. Anisotropic etching of the GaAs wires through their opened ridges generates V-shaped trenches (step iv). Removing the photoresist with acetone leaves clean wires bonded to the PDMS stamp through the SiO<sub>2</sub> stripes (step v). The resultant wires can be collected in a liquid dispersion by etching the SiO<sub>2</sub> stripes with diluted HF solution.

Figure 6 shows SEM images of structures associated with the fabrication of GaAs wires with doublet cross sections. The SEM image in Figure 6A shows a PDMS-supported GaAs wire array with their ridges uncovered with photoresist (i.e., a structure similar to the illustration shown in the bottom-right section of

Figure 5). The continuous bright lines indicate that the photoresist layer on the sharp edge of each GaAs wire is completely removed. The weak contrast on both sides of each bright line indicates that the side walls of the wires are shielded with photoresist. The edge of broken photoresist film (arrow) shows that the thickness of the photoresist film is less than the height of the GaAs wires (500 nm versus 650 nm). Anisotropic etching of this sample in H<sub>3</sub>PO<sub>4</sub>/H<sub>2</sub>O<sub>2</sub>/H<sub>2</sub>O solution splits the single ridge into two separate ridges. Figure 6B shows an assembly of GaAs wires obtained by etching a sample like the one shown in Figure 6A for 25 s. Note the formation of V-shaped trenches. Close observation (inset) reveals that the topography of the V-shaped groove is not uniform or flat. Surface fluctuation might be attributed to the roughness of the side walls of the GaAs wires. The wire indicated by the arrow highlights the wavy surfaces that can occur. Because the roughness of the side walls originates from the edge roughness of the mask stripes,<sup>[12]</sup> the quality of GaAs wires can be further improved by decreasing the width variation of mask stripes along their longitudinal axes. The morphology of wires like those shown in Figure 6B was also mapped using atomic force microscopy (AFM; see Figures 6C and D). The increased lateral dimensions compared to the SEM images are likely due to effects of tip convolution.<sup>[19]</sup> The spacing between the two peaks of doublet cross section can be increased by increasing the etching time. Sufficiently long etching times split an individual wire into two separate wires. Figure 6E shows the result after the sample shown in Figure 6A had been etched for 60 s. This image shows that each GaAs wire with a triangular cross section is transformed into two smaller wires with similar cross sections.

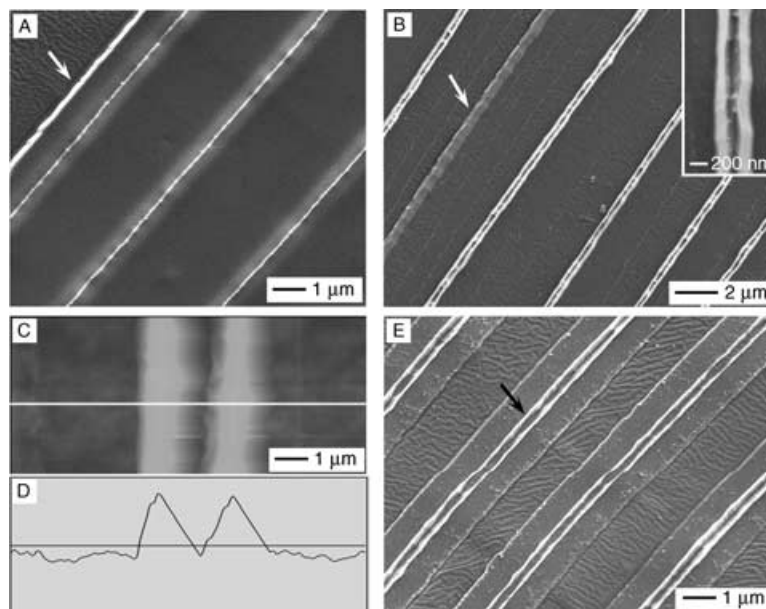


**Figure 6.** Evolution of GaAs wires with a doublet cross section from GaAs wires with a triangular cross section: A) SEM image of triangular GaAs wires embedded in photoresist with only their sharp ridges uncovered; B) SEM and C) AFM images of GaAs wires with doublet cross sections obtained by etching the sample shown in (A) for 25 s; D) Line-cut curve of the AFM image along the white line in (C), revealing the doublet profile; E) SEM image of a sample obtained by etching the sample shown in (A) for 60 s, showing that each GaAs wire can be split into two smaller wires.

In summary, GaAs nanowires with alternating structures along their longitudinal and transverse axes can be prepared, in large-scale amounts, using “top-down” photolithographic procedures and anisotropic etching or deposition. Examples of structures that can be produced easily include GaAs wires with triangular cross sections and alternating widths and compositions along their longitudinal axes, as well as GaAs wires with doublet cross sections. This approach can be extended to the fabrication of nanowires of other semiconductor materials.<sup>[11]</sup> Because the properties of semiconductor nanowires are strongly dependent on their morphology, dimensions, and doping, structures of these types could find applications in various areas that include electronics, photonics, as well as mechanics.

### Experimental Section

Arrays of GaAs wires with triangular cross sections were fabricated using processes reported elsewhere.<sup>[11,12]</sup> For the wires described here, parallel SiO<sub>2</sub> stripes with a width of  $\approx 2 \mu\text{m}$  were defined on a GaAs(100) wafer through traditional photolithography, followed by electron beam evaporation of a SiO<sub>2</sub> thin film and the liftoff of photoresist in hot acetone. The SiO<sub>2</sub> pattern served as an etch mask when GaAs was etched in an aqueous solution of H<sub>3</sub>PO<sub>4</sub>/H<sub>2</sub>O<sub>2</sub>/H<sub>2</sub>O (consisting of 1 volume of H<sub>3</sub>PO<sub>4</sub> (85%), 13 volumes of H<sub>2</sub>O<sub>2</sub> (30%), and 12 volumes of H<sub>2</sub>O) in an ice-water bath. After the SiO<sub>2</sub> mask was removed, the wires retained their order on the wafer because their ends remained in contact with the mother wafer. Parallel photoresist lines with controlled width and spacing were then defined on the wafer perpendicular to the orientation of wires. The photoresist pattern served as a mask for further etching or the deposition of other materials using an electron beam evaporator (Temescal). The resultant wires have alternating lateral dimensions and/or compositions along their longitudinal axes. The wire arrays could also be transferred to a PDMS stamp before the SiO<sub>2</sub> stripes were removed.<sup>[11]</sup> Further operations (as shown in Figure 5) transformed the cross section of the GaAs nanowires from triangular (i.e., single) to doublet profiles.

The SEM images were taken using a field-emission scanning electron microscope (Philips XL 30 ESEM-FEM, FEI) at an accelerating voltage of 10 kV. An electron-dispersive X-ray spectrometer installed on the same microscope was used to analyze and map the elemental compositions of the samples. AFM images were recorded using a Dimension 3100 scanning probing microscope (Digital Instruments) with a silicon nitride tip. The characterization of photoluminescence was performed on a Raman microscope (Kaiser Optical) with confocal imaging mode. A photodiode laser with a wavelength of 785 nm was focused to a spot size of 0.64  $\mu\text{m}$  to illuminate the samples with a power of 5 mW. For plotting each spectrum, the exposure time and number of acquisitions were set as 4 s and 3, respectively.

### Keywords:

chemical etching • nanowires • photolithography • photoluminescence • semiconductors

- [1] a) Y. Xia, P. Yang, Y. Sun, Y. Wu, B. Mayers, B. Gates, Y. Yin, F. Kim, H. Yan, *Adv. Mater.* **2003**, *15*, 353; b) A. P. Alivisatos, P. F. Barbara, A. W. Castleman, J. Chang, D. A. Dixon, M. L. Klein, G. L. McLendon, J. S. Miller, M. A. Ratner, P. J. Rossky, S. I. Stupp, M. E. Thompson, *Adv. Mater.* **1998**, *10*, 1297; c) M. Nirmal, L. Brus, *Acc. Chem. Res.* **1999**, *32*, 407; d) G. Markovich, C. P. Collier, S. E. Henrichs, F. Remacle, R. D. Levine, J. R. Heath, *Acc. Chem. Res.* **1999**, *32*, 415; e) J. Hu, T. W. Odom, C. M. Lieber, *Acc. Chem. Res.* **1999**, *32*, 435.
- [2] a) M. H. Huang, S. Mao, H. Feick, H. Yan, Y. Wu, H. Kind, E. Weber, R. Russo, P. Yang, *Science* **2001**, *292*, 1897; b) M. Law, D. J. Sirbuly, J. C. Johnson, J. Goldberger, R. J. Saykally, P. Yang, *Science* **2004**, *305*, 1269; c) Z. W. Pan, Z. R. Dai, Z. L. Wang, *Science* **2001**, *291*, 1947; d) X. Y. Kong, Y. Ding, R. Yang, Z. L. Wang, *Science* **2004**, *303*, 1348; e) Y. Wang, X. Jiang, Y. Xia, *J. Am. Chem. Soc.* **2003**, *125*, 16176; f) D. Battaglia, J. J. Li, Y. Wang, X. Peng, *Angew. Chem. Int. Ed.* **2003**, *42*, 5035.
- [3] T. Mokari, E. Rothenberg, I. Popov, R. Costi, U. Banin, *Science* **2004**, *304*, 1787.
- [4] a) E. Menard, K. J. Lee, D.-Y. Khang, R. G. Nuzzo, J. A. Rogers, *Appl. Phys. Lett.* **2004**, *84*, 5398; b) X. Duan, C. Niu, V. Sahi, J. Chen, J. W. Parce, S. Empedocles, J. L. Goldman, *Nature* **2003**, *425*, 274; c) E. Menard, R. G. Nuzzo, J. A. Rogers, *Appl. Phys. Lett.* **2005**, *86*, 093057; d) Z. Zhu, E. Menard, K. Hurley, R. G. Nuzzo, J. A. Rogers, *Appl. Phys. Lett.* **2005**, *86*, 133507.
- [5] R. S. Wagner, W. C. Ellis, *Appl. Phys. Lett.* **1964**, *4*, 89.
- [6] M. S. Gudiksen, L. J. Lauhon, J. Wang, D. C. Smith, C. M. Lieber, *Nature* **2002**, *415*, 617.
- [7] M. T. Björk, B. J. Ohlsson, T. Sass, A. I. Persson, C. Thelander, M. H. Magnusson, K. Depper, L. R. Wallenberg, L. Samuelson, *Nano Lett.* **2002**, *2*, 87.
- [8] Y. Wu, R. Fan, P. Yang, *Nano Lett.* **2002**, *2*, 83.
- [9] D. J. Milliron, S. M. Hughes, Y. Cui, L. Manna, J. Li, L.-W. Wang, A. P. Alivisatos, *Nature* **2004**, *430*, 190.
- [10] Y. Wu, J. Xiang, C. Yang, W. Lu, C. M. Lieber, *Nature* **2004**, *430*, 61.
- [11] Y. Sun, J. A. Rogers, *Nano Lett.* **2004**, *4*, 1953.
- [12] Y. Sun, D.-H. Khang, F. Hua, K. Hurley, R. G. Nuzzo, J. A. Rogers, *Adv. Funct. Mater.* **2005**, *15*, 30.
- [13] D. W. Shaw, *J. Electrochem. Soc.*, **1981**, *128*, 874.
- [14] A. Ikehata, T. Itoh, Y. Ozaki, *Anal. Chem.* **2004**, *76*, 6461.
- [15] S. R. Nicewarner-Peña, R. G. Freeman, B. D. Reiss, L. He, D. J. Peña, I. D. Walton, R. Comer, C. D. Keating, M. J. Natan, *Science* **2001**, *294*, 137.
- [16] M. S. Islam, P. J. McNally, *Microelectron. Eng.* **1998**, *40*, 35.
- [17] M. Buda, J. Hay, H. H. Tan, L. Fu, C. Jagadish, P. Reece, M. Gal, *J. Electrochem. Soc.* **2003**, *150*, G481.
- [18] a) J. W. P. Hsu, Y. L. Loo, D. V. Lang, J. A. Rogers, *J. Vac. Sci. Technol. B* **2003**, *21*, 1928; b) C. W. Sheen, J.-X. Shi, J. Martensson, A. N. Parikh, D. L. Allara, *J. Am. Chem. Soc.* **1992**, *114*, 1514.
- [19] M. F. Tabet, F. K. Urban III, *J. Vac. Sci. Technol. B* **1997**, *15*, 800.

Received: March 21, 2005

Revised: June 9, 2005

Published online on September 5, 2005